Investigating the translocation of lambda-DNA molecules through PDMS nanopores

As Published: http://dx.doi.org/10.1007/s00216-008-2529-3

Publisher: Springer Berlin Heidelberg

Persistent URL: http://hdl.handle.net/1721.1/51892

Version: Author's final manuscript: final author's manuscript post peer review, without publisher's formatting or copy editing

Investigating the translocation of λ-DNA molecules through PDMS nanopores

Yi-Heng Sen and Rohit Karnik*

Department of Mechanical Engineering, Massachusetts Institute of Technology, Cambridge, MA 02139.

**Corresponding author: karnik@mit.edu*

Abstract

We investigate the translocation of λ-DNA molecules through resistive-pulse PDMS nanopore sensors. Single molecules of λ-DNA were detected as a transient current increase due to the effect of DNA charge on ionic current through the pore. DNA translocation was found to deviate from a Poisson process when the interval between translocations was comparable to the duration of translocation events, suggesting that translocation was impeded during the presence of another translocating molecule in the nanopore. Characterization of translocation at different voltage bias revealed that a critical voltage bias was necessary to drive DNA molecules through the nanopore. Above this critical voltage, frequency of translocation events was directly proportional to DNA concentration and voltage bias, suggesting that transport of DNA from the solution to the nanopore was the rate limiting step. These observations are consistent with experimental results on transport of DNA through nanopores and nanoslits, and the theory of hydrodynamically driven polymer flow in pores.

Keywords

Nanopore, DNA, resistive-pulse, biosensing, PDMS, translocation.

Introduction

Nanopores have emerged as versatile sensors for detection and analysis of single molecules and particles over the past decade [1-7]. Similar to Coulter counters, nanopores employ resistive pulse sensing in which ionic current through the pore changes during translocation (passage) of a molecule through the pore [2]. Particularly, attention has been focused on developing nanopores for rapid sequencing of DNA using α-hemolysin and solid-state nanopores [1]. While close interactions between the nanopore and the DNA molecule can yield structural information about the molecule, larger nanopores in the 10-500 nm size range are better suited for analysis of physicochemical characteristics. Saleh and Sohn [4] used rapid prototyping in PDMS (polydimethylsiloxane) to fabricate 200-400 nm nanopores for detection of λ-DNA, while Fan et al. [5] used silica nanotubes for sensing λ-DNA. While larger nanopores are relatively easy to fabricate, the signal-to-noise ratio is compromised due to the large size of the nanopore. To address this issue, we are developing devices to perform multiple measurements on long DNA molecules, which could significantly improve the signal-to-noise ratio by statistical averaging on the same molecule [8, 9].

Knowledge of the factors that affect the frequency of translocation events is critical for designing such nanopore devices and for understanding the mechanisms that govern transport of these molecules through the nanopore. Study of DNA translocation through α-hemolysin nanopores [10, 11] and solid-state nanopores [12] has yielded valuable insights into the effect of voltage bias, DNA concentration, DNA length, etc. on the translocation frequency, duration, and current blockage. However, relatively little is known about translocation of long DNA molecules through larger nanopores that involve a significantly different pore geometry, size, and electric fields. In this paper, we examine the effects of voltage bias and DNA concentration on the translocation of λ-DNA through PDMS nanopores.

Background

Change of ionic current during translocation of DNA

Translocation of a charged molecule such as λ-DNA through a pore can affect the ionic current through (a) change of the effective ionic concentration in the nanopore due to charges carried by the molecule, and (b) blockage of nanopore with λ-DNA [5, 13, 14]. Since DNA is negatively charged, additional conducting counterions are introduced into the pore when the molecule enters a nanopore, resulting in an increase in the ionic current ΔI_{charge} given by [5, 13, 15]

$$\Delta I_{charge} = \mu b \Delta n e V / L_{pore}^2 \quad (1)$$

where Δn is the number of charges introduced uniformly into a nanopore of length L_{pore} with a voltage bias V applied across it, e is charge of an electron, μ is ionic mobility, and b is the fraction of counterions that are mobile [13]. This mechanism dominates at low ionic concentrations, where the total number of ions in the bulk solution is small. At higher buffer concentrations, physical blockage of the nanopore by the DNA molecule dominates, resulting in a current decrease during translocation given by [16]:

$$\Delta I_{block} / I = V_{particle} / V_{pore} \quad (2)$$

where ΔI_{block} is current change, I is to open pore ionic current, and $V_{particle}/V_{pore}$ is the ratio of particle to pore volume. For sensing DNA in a KCl solution, these two competing effects cancel at a concentration of ~0.37 M [14]. Thus, current transiently increases during translocation at KCl concentrations below this value, while it decreases during translocation at KCl concentrations above this value.

Translocation of DNA molecules through nanopores

A single translocation event involving the transport of DNA molecules from a solution on one side of the nanopore to the other side may be sub-divided into three steps [11, 17]: (a) transport of DNA molecules from the solution to the opening of the nanopore, (b) entrance of the molecule into the nanopore, and (c) translocation of the molecule across the nanopore to the solution on the other side. Transport of DNA molecules to the nanopore may occur by diffusion, electrokinetic transport, or by convection. The frequency of arrival of the molecules at the entrance of the nanopore is linearly proportional to the DNA concentration and the electric field at the entrance [10] given by $1/\tau_{arr} \propto c \times V$, where $1/\tau_{arr}$ is the frequency of DNA arrival at the pore entrance, c is the DNA concentration, and V is the applied voltage bias. Entrance of the DNA molecule into the nanopore requires crossing an entropic free energy barrier since the DNA conformation is constrained inside the nanopore when the pore size is smaller than DNA size. The timescale for translocation depends exponentially on the voltage bias and free energy barrier [18] as $1/\tau_{ent} \propto \exp(zeV - \Delta G^* / kT)$, where z is the number of charges that interact with the electric field, V is potential difference in the entrance region of the pore, and ΔG^* is the free energy barrier. Translocation of the DNA molecule across the nanopore depends on the applied voltage bias and the mobility of DNA molecules through the nanopore [10], given by $1/\tau_{trans} \propto V$.

The actual frequency of the translocation events will depend on which of the above steps is rate limiting. Translocation frequency of oligonucleotides through α-hemolysin pores has been observed to increase exponentially with voltage bias for low bias, suggesting that entrance into the pore was rate limiting step [11, 18]. At high voltage bias, the dependence on voltage bias grew weaker and the translocation frequency was comparable to capture rate, suggesting that intermolecular interactions limited the frequency of translocation[11]. The transport of long DNA molecules through nanoscale slits was found to be limited by transport of DNA to the slit for high voltage bias, while it was limited by entrance into the slit for low voltage bias. [17, 19].

Scaling relations describing transport of polymers through pores

Performing a scaling analysis for hydrodynamically driven transport of polymers through pores, Daoudi et al. [20] showed the existence of a critical fluid current density (J_c) that is independent of polymer length, polymer concentration (for dilute solutions), and pore diameter, above which polymers can be forced into the pore. Above the polymer overlap concentration, the critical fluid current decreases rapidly as $c^{-15/4}$ as repulsive intermolecular interactions enable the polymers to enter the pore more easily. In the

absence of nonlinear electrokinetic effects, the electric field distribution is similar to the fluid current distribution at the entrance of the pore, and we can expect similarity between hydrodynamically driven polymer translocation and electrically driven DNA translocation.

Experimental section

Device fabrication

Nanopore devices were fabricated using rapid prototyping in PDMS [21] from a master mold, followed by plasma bonding to a glass substrate. The master mold was fabricated on a silicon wafer using e-beam lithography to pattern titanium (Ti) metal lines that defined the nanopore. Ti lines were patterned using the lift-off technique with a thickness of 200 nm, widths ranging from 200 to 500 nm, and lengths ranging from 5 to 8 μm. Subsequently, 10 μm thick SU-8 photoresist was patterned on the silicon wafer to define the connecting microfluidic channels. This two-step procedure resulted in a master mold with metal lines defining nanochannels and SU-8 defining the microfluidic channels. To aid removal of PDMS from the mold, the wafer was placed overnight in a desiccator with a few drops of tridecafluoro-1,1,2,2-tetrahydrooctyl-1-trichlorosilane (United Chemical Technologies). PDMS monomer and curing agent (Sylgard 184, Dow Corning) were mixed in a ratio of 10:1 as specified by the manufacturer and poured on the mold. The device was cured for 2 days at 80 ºC and removed from the mold, following which holes were punched to create the input and output reservoirs. Subsequently, the PDMS component was cleaned with ethanol and isopropanol and bonded to a clean glass slide using oxygen plasma to result in the nanopore device (Figure 1). DNA solution was introduced into the device immediately after plasma bonding. Once fabricated, the device was robust, allowing for hours of measurement.

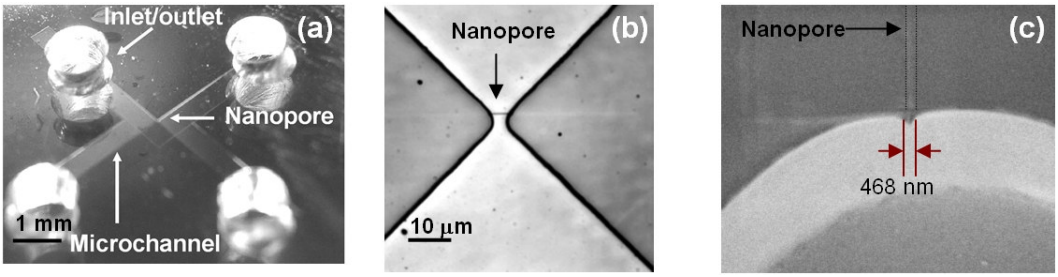

Figure 1. PDMS nanopore device. (a) Device showing inlet and outlet reservoirs, and connecting microchannels. (b) Micrograph of the device showing a 200 nm × 500 nm × 5 μm nanopore with microchannels on either side. (c) SEM image showing the PDMS component before bonding. The trough corresponding to the nanopore is outlined for clarity.

Experimental setup

The PDMS nanopore sensor device comprised two microfluidic channels with reservoirs at either end of the channels, with a nanopore connecting the two

microchannels. Ag/AgCl (In Vivo Metric) electrodes were inserted into one of the reservoirs of each microchannel for making electrical contact with the solution. Axopatch 200B patch clamp amplifier (Axon Instruments, Union City, CA) was used to apply a voltage bias and measure the corresponding ionic current through the nanopore. Current measurements were taken inside a Faraday cage to shield from any electromagnetic interference. The current I_{pore} through the nanopore was filtered by a low-pass Bessel filter (80 dB/decade) at 1 kHz cutoff frequency embedded in the amplifier. The Axopatch instrument output a voltage signal V_I, corresponding to the nanopore current, which was digitized at 20 kHz/16 bits using a Data Acquisition Card (DAQ) (PCI-6251M, National Instruments, Austin, TX) installed on a desktop computer and controlled by a home-built Labview program (National Instruments). The Labview program supplied a voltage V_v to the Axopatch amplifier, which then applied a proportional voltage V_{pore} across nanopore. The maximum output voltage of the Aoxpatch/LabVIEW setup was 1 V, while the maximum measurable current with low measurement noise was 10 nA.

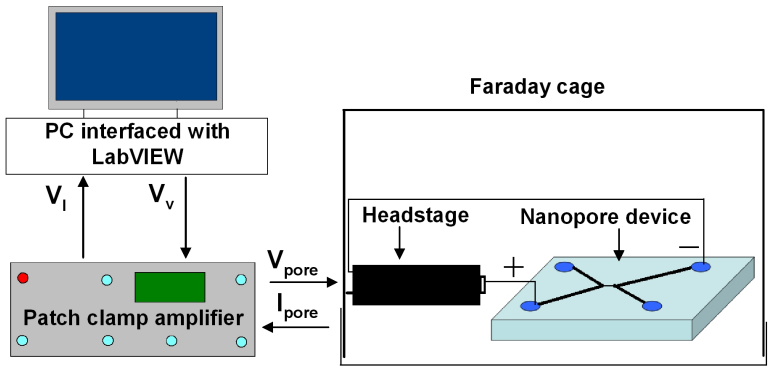

Figure 2. Experimental setup for measuring the translocation of DNA through a PDMS nanopore device.

Materials

48.5 kbp long λ-DNA (10 mM Tris-HCl pH 8.0, 1 mM EDTA) was purchased from New England BioLabs, Inc., and dissolved in 10 mM KCl buffer solution before use. Bovine serum albumin (BSA, Sigma Aldrich), was dissolved in 10 mM KCl solution, and filtered with a 0.2 µm syringe filter (VWR International, Inc.) before introducing into the device.

Data analysis

Data analysis was implemented using Matlab R14 (The MathWorks, Natick, MA). Data was acquired at 20 kHz and was subsequently digitally filtered by a moving average method over a window of 1 ms (Figure 3). Digitally filtered current traces are presented throughout this paper except for Figures 3a and b, where unprocessed data is shown for comparison.

The events of DNA entry and escape out of the nanopore were determined by monitoring the rate of change of current with time. A DNA entry event was identified by setting a threshold value for current change (2-4 pA) in a given window of time (12-14

ms). The number of entry events was used to construct the histograms in Figure 6. The histograms in Figure 9 were constructed by eliminating all events from the histograms in Figure 9 that occurred within the average translocation time t_0 of the previous event (data was not re-processed). Scatter plots of translocation duration and current signal amplitude were obtained by setting additional criteria to determine escape time and to ensure that only single translocation events were counted. The escape of a DNA molecule was determined by setting a threshold criterion of current increase for stabilization of the current in a 12 ms time window after a specified delay following an entry event. Translocation events were considered only if one entrance event preceded an escape event, which excluded all translocation events with multiple peaks that comprised between 25 to 40% of all entrance events. The entry and escape times were marked on the plot of current vs. time, and examined manually for all processed data to ensure accuracy of the algorithm. However, translocation events were manually counted in the case of 8 μm long nanopores (Figure 11) where an automated algorithm resulted in significant errors.

Results and discussion

Detection of DNA translocation in PDMS nanopores

The change in ionic current due to translocation of DNA depends on the ionic concentration. The change in current at high KCl concentration is dominated by blockage of the nanopore, Eqn. (2) predicts a current change in the range of 1 pA for a pore current of 10 nA, the maximum current that the instrument can measure with a very low noise level. On the other hand, Eqn. (1) predicts the corresponding current increase at low KCl concentrations to be in the range of 10-15 pA under a voltage bias of 1 V, giving much better detection capability and signal to noise ratio at lower KCl concentrations. However, effects of surface charge start dominating as the ionic concentration is decreased, which can lead to undesirable current transients and nonlinear electrokinetic effects during measurement. We therefore picked a moderately low concentration of 10 mM KCl for detection of DNA in our device. To verify that translocation of λ-DNA could be detected, a 10 μg/mL solution of λ-DNA in 10 mM KCl was introduced on one side of a 200 nm × 500 nm × 5 μm nanopore, while only 10 mM KCl solution was introduced on the other side of the pore. When a voltage bias of 0.5 V was applied such that the DNA side was negatively biased, transient current signals were observed indicating DNA translocation events (Figure 3a).

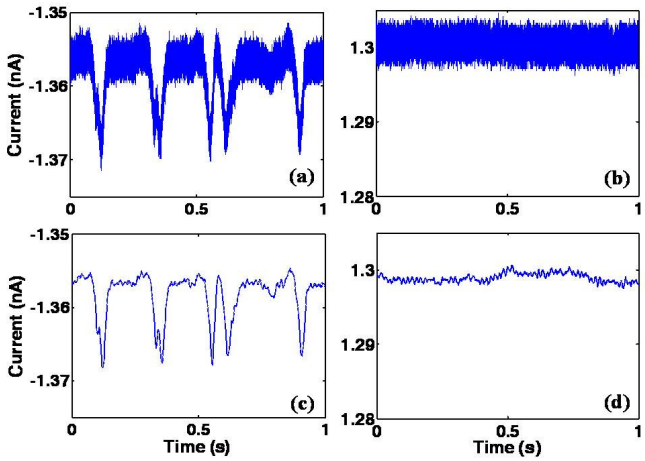

Figure 3. (a) Transient changes in ionic current through a 200 nm × 500 nm × 5 μm nanopore during translocation of λ-DNA. (10 μg/mL λ-DNA in 10 mM KCl, voltage bias 0.5 V). (b) No translocation signals were observed when the voltage polarity was reversed. (c) and (d) Digital filtering of the current traces in (a) and (b) with a moving average over a window of 1 ms yields higher signal-to-noise ratios for the translocation signals.

All translocation signals had similar peak heights of ~14 pA, and durations of ~50 ms, over a baseline current of 1.35 nA (Figure 3). With an ionic mobility of 7.9×10^{-8} m^2/Vs for potassium and chloride ions, $b = 0.5$, and $\Delta n = 48500\times2 = 97000$, Eqn. (2) predicts a current increase of about 12 pA assuming that the entire DNA molecule is within the nanopore. While the fully stretched length of λ-DNA is about 16 μm, we expect the molecule to be only partially stretched as the nanopore cross-section is larger than the persistence length of double-stranded DNA. Furthermore, the DNA molecule may enter the nanopore in a folded conformation, and we therefore expect that a significant portion of the molecule will be inside the 5 μm long nanopore during translocation. Thus, the measured peak heights of the current signals agree with the expected change in the current through the nanopore during translocation. Furthermore, the translocation duration of 50 ms is in agreement with the 2-10 ms duration of λ-DNA translocation through 200 nm × 200 nm × 3 μm PDMS nanopores [4] and the 5-20 ms duration for 3 μm long, 50-100 nm diameter silica nanotubes [5]. We expect longer translocation duration due to the fact that our nanopore is longer, leading to a smaller electric field along the nanopore for the same applied voltage bias. Furthermore, the transient signals observed in our device disappeared when the voltage bias was reversed (Figure 3b), or when KCl solution without any DNA was introduced into the device, confirming that the observed signals were due to translocation of single molecules of λ-DNA through the nanopore.

Passivation of the nanopore with BSA for enhanced stability

While current signals due to DNA translocation were evident in the nanopore device, the baseline current was not stable under continuous voltage bias with translocation of λ-DNA through the nanopore. We observed that baseline current exhibited large fluctuations and an overall increase in magnitude over time during the measurement

process (Figure 4). Since the baseline current remained stable (except for effects of evaporation) in the absence of DNA, it suggested the possibility that DNA molecules might be accumulating inside the nanopore, effectively increasing the number of ions in the pore due to their charge. We therefore explored the possibility of coating the nanopore with bovine serum albumin (BSA) to improve the device stability by preventing aggregation of DNA molecules inside the nanopore. 1 mg/mL of BSA in 10 mM KCl buffer was introduced into the device for 10 min, followed by rinsing with deionised water before introduction of DNA. Indeed, we observed that the baseline current was very stable in the BSA-coated nanopores as compared to uncoated nanopores. Experiments could be performed on the coated nanopores for ~1 h before the baseline current again became unstable. This time may correspond to the slow escape of BSA molecules out of the nanopore, which may be augmented by the electric field due to the applied voltage bias. DNA translocation signals and the baseline current were similar to those in the uncoated nanopores, which suggest that adsorption of BSA on the walls of the nanopore prevented aggregation of λ-DNA inside the pore, but otherwise did not significantly affect DNA translocation.

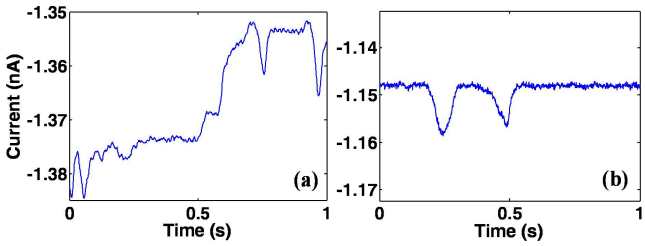

Figure 4. (a) Nanopore devices were not very stable and exhibited sudden changes in baseline current, likely due to accumulation of DNA molecules inside the nanopore. (b) Passivation of the nanopore with BSA prevented this phenomenon and resulted in a stable baseline current (200 nm × 500 nm × 5 μm nanopore, 10 μg/mL λ-DNA in 10 mM KCl, voltage bias 0.5 V).

Characterization of DNA translocation

Comparison of DNA translocation with a Poisson process

In the case of DNA translocation through nanopores with minimal interactions between the DNA molecules, we expect that the translocation events will follow a Poisson process[11]. However, any interactions between the molecules may cause deviations from this ideal behavior. We therefore examined the translocation process by studying the *inter-translocation* time T defined as the time interval between the *starts* (entry) of two consecutive DNA translocation events (Figure 5). Figure 6 shows histograms of the inter-translocation time for λ-DNA passing through a 200 nm × 500 nm × 5 μm nanopore under different applied voltages ranging from 0.5 to 1 V, measured over periods of 79 s. The number of DNA translocation events increased significantly from 2.2 s^{-1} at 0.5 V to 5.1 s^{-1} at 1 V, while the mean inter-translocation time decreased concomitantly from 0.45 s to 0.20 s. For a Poisson process, the interval between arrivals (corresponding to the inter-translocation time) has an exponential distribution. Clearly,

the inter-translocation time exhibited a maximum and did not obey the Poisson distribution, with the deviation being more evident at lower voltage bias (Figure 6).

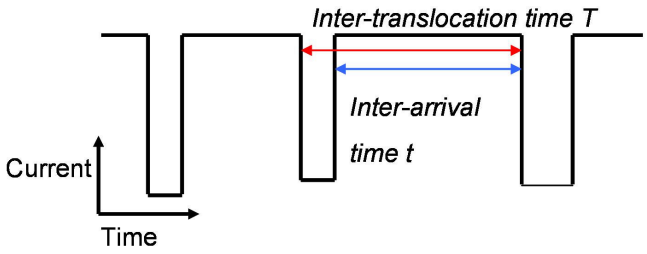

Figure 5. Schematic diagram illustrating the definitions of inter-translocation time (T, marked in red) and inter-arrival time (t, marked in blue).

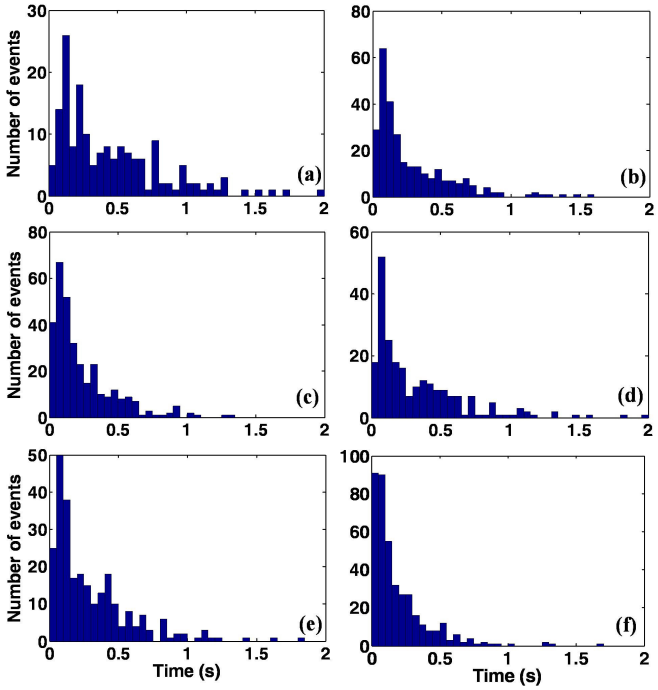

Figure 6. Histograms of DNA inter-translocation time T with voltage bias of 0.5 V (a), 0.6 V (b), 0.7 V (c), 0.8 V (d), 0.9 V (e), and 1 V (f). Each histogram was obtained from a measurement of translocations in a period of 79 s (200 nm × 500 nm × 5 μm nanopore, 5 μg/mL λ-DNA in 10 mM KCl, each bar represents 50 ms).

To gain insight into this process, we examined the durations and signal amplitudes of the translocation events (Figure 7). When the translocations of two DNA molecules overlap, the number of translocation events can be counted but their durations cannot be accurately estimated. These events were therefore omitted from the scatter plots, and only those events that had a single peak were considered. A remarkable trend emerged with increasing voltage bias: At a voltage bias of 0.5 V, there was no correlation between the signal amplitude and the translocation duration, but a clear correlation emerged with increasing voltage bias where the signal amplitude was higher for longer translocation

durations. This observation suggests two likely interpretations: It is possible that at higher voltage bias compact conformations of the DNA molecule can translocate through the nanopore, which will result in larger signal amplitude. However, a larger translocation time requires that these conformations have lower mobility than the conformations that dominate at lower voltage bias. The second possibility is that the chance of multiple molecules translocating through the nanopore increases at a higher voltage bias. This results in larger signal amplitude as well as longer translocation duration. However, the mean translocation time at 1 V bias was 54 ms, which is slightly less than half of the mean translocation time of 121 ms at 0.5 V bias, showing that the mobility is approximately constant. Therefore, we conclude that the most likely reason for our observations is that multiple molecules are more likely to translocate through the nanopore at higher voltage bias. A closer look at the histogram in Figure 6 shows that the deviation from the Poisson process was more evident at lower voltage bias. Furthermore, translocation signals with large current amplitudes (several times that of the average amplitude) that would be observed if the translocation events were Poisson, are completely absent. In combination with the other results, it suggests that interactions between DNA molecules are effective in excluding other DNA molecules during translocation at a lower voltage bias, which results in larger deviation from the Poisson distribution for inter-translocation time (Figure 6). We expect that translocation of a DNA molecule through the nanopore may increase the barrier to entry for a second DNA molecule. This barrier may be entropic in origin, requiring change in conformation of the molecules to accommodate two molecules instead of one molecule. It is possible that a low voltage bias is insufficient to enable the second DNA molecule to overcome this barrier and enter the pore simultaneously with the first molecule, resulting in exclusion of the DNA molecules. A higher applied voltage bias may be sufficient to overcome this extra barrier, enabling a DNA molecule to enter the nanopore during the translocation of another molecule, resulting in simultaneous translocation of multiple molecules through the nanopore. To verify that the observed signals were indeed due to translocation of multiple molecules through the nanopore, we examined DNA translocation at a lower concentration (1 μg/mL) with a high voltage bias of 1 V. Figure 8 compares the scatter plots of current change and translocation duration for DNA translocation with a voltage bias of 1V at 1 μg/mL (black dots) and 5 μg/mL (red dots). A strong correlation between signal amplitude and translocation duration was seen at a concentration of 5 μg/mL, while there was little correlation between signal amplitude and translocation duration in 1 μg/mL. Thus, the effect disappeared at low DNA concentrations, verifying that the origin of the correlation between signal amplitude and translocation duration was due to simultaneous translocation of multiple DNA molecules.

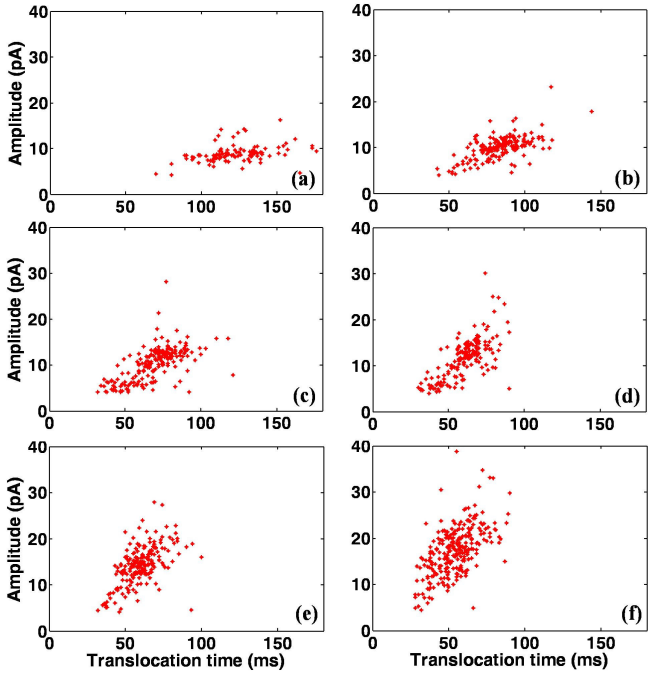

Figure 7. Scatter plots of DNA translocation time and signal amplitude with voltage bias of 0.5 V (a), 0.6 V (b), 0.7 V (c), 0.8 V (d), 0.9 V (e), and 1 V (f) corresponding to histograms in Figure 6. Each plot was obtained from a measurement of translocations in a period of 79 s (200 nm × 500 nm × 5 μm nanopore, 5 μg/mL λ-DNA in 10 mM KCl, each bar represents 50 ms).

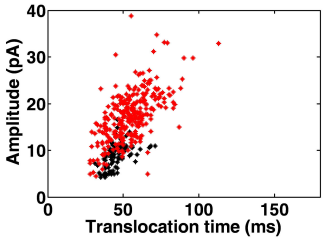

Figure 8. Scatter plots of DNA translocation time and signal amplitude with voltage bias of 1 V at DNA concentrations of 5 μg/mL (red dots) and 1 μg/mL (black dots).

While entry of DNA molecules into the nanopore may be impeded during translocation of another molecule, the process must be Poisson in the absence of any translocating molecule. We therefore verified whether DNA translocation event through the nanopore *after* a previous DNA translocation has been completed was a Poisson process [22]. Here the inter-arrival time t is defined as time interval between the *completion* of the last DNA translocation and the *start* of a subsequent translocation (Figure 5). Thus, t is equal to the length of inter-translocation time T minus the DNA translocation time t_0. In other words, we tried to verify whether the distribution of translocation inter-arrival time t would be the same as the inter-arrival time in a Poisson process. The probability density function of inter-arrival time in the Poisson process is $f(t) = \lambda e^{-\lambda t}$, where λ is the average value of inter-arrival time. Since $T = t + t_0$, the probability that inter-translocation time T ($T \geq t_0$) falls between $t_0 + t_1$ and $t_0 + t_2$ is:

$$P(t_1 + t_0 \le T \le t_2 + t_0) = e^{-\lambda t}\,|_{t=t_1} - e^{-\lambda t}\,|_{t=t_2} \qquad (4)$$

Moreover, since the average DNA translocation time t_0 decreased with the increase of voltage, the minimum inter-translocation time (T_{min} = t_0) for which we extracted the events increased with the decrease of voltage. From the scatter plot (Figure 7) for different magnitudes of voltage, the average translocation time t_0 was 121 ms for 0.5 V, 83.9 ms for 0.6 V, 69.2 ms for 0.7 V, 60.5 ms for 0.8 V, 60.2 ms for 0.9V, and 54 ms for 1 V. Figure 9 shows the histogram of the inter-arrival time and the theoretical curve corresponding to a Poisson process calculated from Eqn. (4). The inter-arrival time corresponds closely to the inter-arrival time in a Poisson process, showing that DNA translocation was indeed a Poisson process when there was no molecule translocating through the nanopore.

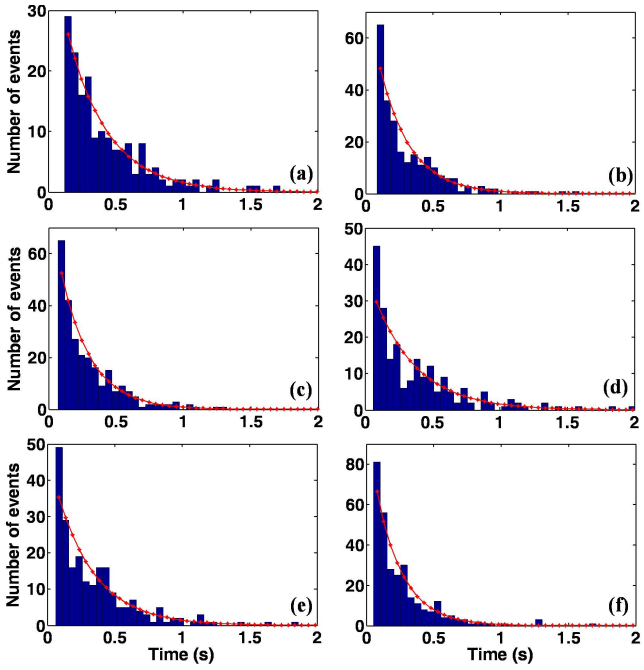

Figure 9. Histograms of DNA inter-translocation time T of events in Figure 6 showing events that occurred after the average translocation time t_0 had elapsed since the last translocation. Applied voltage bias was 0.5 V (a), 0.6 V (b), 0.7 V (c), 0.8 V (d), 0.9 V (e), and 1 V (f). Each bar represents a time interval of 50 ms, with the first bar starting at $t = t_0$ to $t = t_0 + 50$ ms.

Critical voltage bias is required for DNA translocation

The frequency of translocation events is expected to depend exponentially on the applied voltage bias when the rate limiting step is the entrance of the molecule into the nanopore [11, 17]. Theory of polymer flow through pores also predicts that a critical driving current or flow is required for the DNA to enter the nanopore. Furthermore, this critical current is expected to decrease rapidly with concentration when interactions between DNA molecules become significant [23]. We therefore explored the effect of DNA concentration and applied voltage bias on the frequency of translocation events

through a nanopore. Figure 10 compares the current traces for a 200 nm × 500 nm × 5 μm nanopore for the same DNA concentration (5 μg/mL) at a voltage bias of 0.5 V with a bias of 0.4 V. While translocation signals were clearly evident at a bias of 0.5 V, no translocation events were detected at a voltage bias of 0.4 V. We compared the frequency of DNA translocations at different DNA concentrations in another nanopore device (Figure 11). The frequency of DNA translocations decreased linearly with the applied voltage for all the measured concentrations, and abruptly decreased to zero below a certain critical voltage. The critical voltage increased with increasing DNA concentration. Now, the DNA overlap concentration c^* beyond which significant overlap is expected is in the range of 30-50 μg/mL in the case of λ-DNA, but the behavior starts deviating from that of a dilute solution beyond a concentration of 5 μg/mL [24]. Since the DNA concentrations we used were all well below overlap concentration, we observed that critical ionic current and therefore the critical voltage did not show a large dependence ($c^{-15/4}$) on concentration that is expected when $c>c^*$. However, a mild dependence of the critical voltage on DNA concentration was evident, with the critical voltage decreasing from about 0.3 V to 0.2 V as the DNA concentration increased from 0.625 to 7.5 μg/mL.

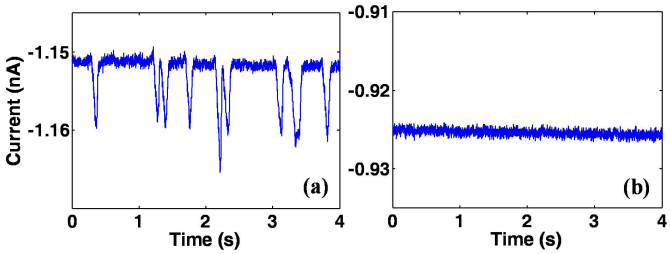

Figure 10. Comparison of current through a nanopore at a voltage bias of 0.5 V (a) and at voltage bias of 0.4 V (b) under identical conditions. (200 nm × 500 nm × 5 μm nanopore, 5 μg/mL λ-DNA).

In addition, we observed a linear relationship between magnitude of voltage and frequency of translocation events. This could be the result of increased electric field in the vicinity of the nanopore entrance that causes a linear increase in arrival rate [11], or due to electro-osmotic flow that also increases linearly with the applied voltage. This linear dependence and critical voltage suggest that the translocation frequency was dominated by the transport of DNA to the nanopore.

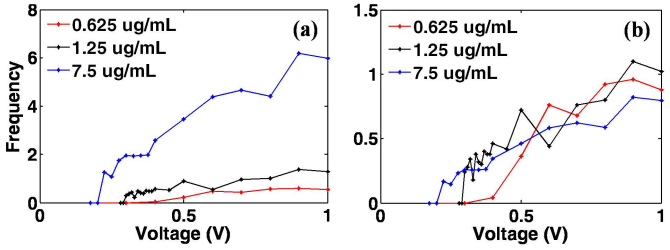

Figure 11. (a) Frequency of DNA translocation events with different voltage bias and DNA concentrations. Blue line represents DNA concentration of 7.5 μg/mL, black line represents DNA concentration of 1.25 μg/mL, and red line represents DNA concentration of 0.625 μg/mL. (b) Event frequency normalized with DNA concentration. The frequency of translocation (average number of translocation events per second) was obtained by measuring over a 40 s interval.

Conclusion

In this paper we focused on characterizing the translocation of single 48.5 kbp λ-DNA molecules through an artificial PDMS nanopore. 48.5 kbp λ-DNA molecules in 10 mM KCl were successfully detected in PDMS nanopore with 200 nm × 500 nm cross section and 5-8 μm length. The translocation durations and current amplitudes showed good agreement with simple electrokinetic models and previous work on detection of λ-DNA in nanopores with similar dimensions. Stability of the current signal was greatly improved by coating the nanopore with BSA. Factors such as applied voltage bias, DNA concentration, and dimensions of the channel were found to affect the frequency of translocation events. Our experiments reveal that intermolecular interactions can be significant within the range of DNA concentrations reported in the literature [4, 5], and show the existence of a critical driving voltage that is necessary for the translocation of DNA molecules across the nanopore. We drew an analogy between electrically driven DNA translocation through nanopores and the forcing of polymers through pores [23], which also predicts a critical driving force for translocation.

PDMS nanopores are easy to fabricate and integrate with microfluidic devices. The ability to detect single molecules and particles in microfluidic devices that can perform sample processing would be advantageous for operations such as DNA fragment sizing, sensing, and analysis following PCR or enzymatic digestion. We are developing a nanopore system that can perform multiple measurements on single DNA molecules, which would enable accurate integrated sizing of DNA fragments and nanoparticles without the need for fluorescence microscopy and image processing [9]. This approach may enable stand-alone devices for integrated analysis of nanoparticles, viruses, and large DNA fragments that typically requires optical equipment. Our results may help the future development and design of such devices for integrated analysis of single molecules and particles.

Acknowledgements

Devices were fabricated at MIT's Microsystems Technology Laboratory and the SEBL facility at the Research Laboratory of Electronics. We acknowledge financial support from the Karl Chang Innovation Award.

References

1. Deamer DW, Akeson, M. (2000) Trends in Biotech. 18:147-151
2. Bayley H, Martin CR (2000) Chemical Reviews 100:2575-2594
3. Kasianowicz J, Brandin E, Branton D, Deamer D (1996) PROCEEDINGS OF THE NATIONAL ACADEMY OF SCIENCES OF THE UNITED STATES OF AMERICA 93:13770-13773
4. Saleh O, Sohn L (2003) Nano Lett 3:37-38
5. Fan R, Karnik R, Yue M, Li DY, Majumdar A, Yang PD (2005) Nano Lett 5:1633-1637
6. Siwy Z, Trofin L, Kohli P, Baker LA, Trautmann C, Martin CR (2005) J Am Chem Soc 127:5000-5001
7. Storm AJ, Chen JH, Ling XS, Zandbergen HW, Dekker C (2003) Nature Materials 2:537-540
8. Gershow M, Golovchenko JA (2007) Nature Nanotechnology 2:775-779
9. Sen Y-H, Karnik R (2008) Proceedings of Micro Total Analysis Systems, San Diego, CA
10. Chen P, Gu JJ, Brandin E, Kim YR, Wang Q, Branton D (2004) Nano Lett 4:2293-2298
11. Meller A, Branton D (2002) Electrophoresis 23:2583-2591
12. Storm AJ, Storm C, Chen JH, Zandbergen H, Joanny JF, Dekker C (2005) Nano Lett 5:1193-1197
13. Chang H, Kosari F, Andreadakis G, Alam M, Vasmatzis G, Bashir R (2004) Nano Lett 4:1551-1556
14. Smeets RMM, Keyser UF, Krapf D, Wu MY, Dekker NH, Dekker C (2006) Nano Lett 6:89-95
15. Karnik R, Castelino K, Fan R, Yang P, Majumdar A (2005) Nano Lett 5:1638-1642
16. Saleh OA, Sohn LL (2001) Review of Scientific Instruments 72:4449-4451
17. Han J, Turner SW, Craighead HG (1999) Phys Rev Lett 83:1688-1691
18. Henrickson SE, Misakian M, Robertson B, Kasianowicz JJ (2000) Phys Rev Lett 85:3057-3060
19. Han J, Craighead H (2000) SCIENCE 288:1026-1029
20. Daoudil SB, F. (1978) Macromolecules *11*:751 - 758
21. Duffy DC, McDonald JC, Schueller OJA, Whitesides GM (1998) Analytical Chemistry 70:4974-4984
22. Drake AW (1967) Fundamentals of applied probability theory. McGraw-Hill
23. Daoudi S, Brochard F (1978) Macromolecules 11:751-758
24. Verma R, Crocker JC, Lubensky TC, Yodh AG (1998) Phys Rev Lett 81:4004-4007